JCI The Journal of Clinical Investigation

Human-derived neural progenitors functionally replace astrocytes in adult mice

Hong Chen, … , Melvin Ayala, Su-Chun Zhang

J Clin Invest. 2015. https://doi.org/10.1172/JCI69097.

Technical Advance **Neuroscience**

Astrocytes are integral components of the homeostatic neural network as well as active participants in pathogenesis of and recovery from nearly all neurological conditions. Evolutionarily, compared with lower vertebrates and nonhuman primates, humans have an increased astrocyte-to-neuron ratio; however, a lack of effective models has hindered the study of the complex roles of human astrocytes in intact adult animals. Here, we demonstrated that after transplantation into the cervical spinal cords of adult mice with severe combined immunodeficiency (SCID), human pluripotent stem cell–derived (PSC-derived) neural progenitors migrate a long distance and differentiate to astrocytes that nearly replace their mouse counterparts over a 9-month period. The human PSC-derived astrocytes formed networks through their processes, encircled endogenous neurons, and extended end feet that wrapped around blood vessels without altering locomotion behaviors, suggesting structural, and potentially functional, integration into the adult mouse spinal cord. Furthermore, in SCID mice transplanted with neural progenitors derived from induced PSCs from patients with ALS, astrocytes were generated and distributed to a similar degree as that seen in mice transplanted with healthy progenitors; however, these mice exhibited motor deficit, highlighting functional integration of the human-derived astrocytes. Together, these results indicate that this chimeric animal model has potential for further investigating the roles of human astrocytes in disease pathogenesis and repair.

Human-derived neural progenitors functionally replace astrocytes in adult mice

Hong Chen,[1,2] Kun Qian,[2] Wei Chen,[2] Baoyang Hu,[2] Lisle W. Blackbourn IV,[2] Zhongwei Du,[2] Lixiang Ma,[2] Huisheng Liu,[2] Karla M. Knobel,[2] Melvin Ayala,[2] and Su-Chun Zhang[2,3]

[1]Department of Rehabilitation of Tongji Hospital, Tongji Medical College, Huazhong University of Science and Technology, Wuhan, China. [2]Waisman Center and [3]Department of Neuroscience and Department of Neurology, University of Wisconsin, Madison, Wisconsin, USA.

Astrocytes are integral components of the homeostatic neural network as well as active participants in pathogenesis of and recovery from nearly all neurological conditions. Evolutionarily, compared with lower vertebrates and nonhuman primates, humans have an increased astrocyte-to-neuron ratio; however, a lack of effective models has hindered the study of the complex roles of human astrocytes in intact adult animals. Here, we demonstrated that after transplantation into the cervical spinal cords of adult mice with severe combined immunodeficiency (SCID), human pluripotent stem cell–derived (PSC-derived) neural progenitors migrate a long distance and differentiate to astrocytes that nearly replace their mouse counterparts over a 9-month period. The human PSC-derived astrocytes formed networks through their processes, encircled endogenous neurons, and extended end feet that wrapped around blood vessels without altering locomotion behaviors, suggesting structural, and potentially functional, integration into the adult mouse spinal cord. Furthermore, in SCID mice transplanted with neural progenitors derived from induced PSCs from patients with ALS, astrocytes were generated and distributed to a similar degree as that seen in mice transplanted with healthy progenitors; however, these mice exhibited motor deficit, highlighting functional integration of the human-derived astrocytes. Together, these results indicate that this chimeric animal model has potential for further investigating the roles of human astrocytes in disease pathogenesis and repair.

Introduction

Astrocytes comprise the largest cell population in the vertebrate CNS. In the adult CNS, each astrocyte and its processes occupy discrete domains, insulating neurons and up to 10^5 synapses and regulating synaptic activity (1, 2). Astrocytes connect to each other through gap junctions and participate in the formation and maintenance of the blood-brain barrier through their end feet encircling endothelial cells of blood vessels, thus coupling neuronal activities with metabolism in the homeostatic CNS (3, 4).

Astrocytes are also active participants in neurological conditions. In a rare disorder of astrocytes, Alexander disease, mutations in the glial fibrillary acidic protein (GFAP) lead to a cascade of astrocyte dysfunction, neuronal degeneration, and leukodystrophy (5), highlighting the critical roles of astrocytes in maintaining the homeostasis of the CNS as well as pathogenesis of neurological conditions. Astrocytes derived from transgenic animals or patients with neurological disorders, such as ALS, Rett syndrome, and Huntington disease, appear to damage neurons in coculture (6–9) or after transplantation (10). Hence, astrocytes play important roles in disease progression and may also be potential targets for therapeutic intervention (11).

Evolutionarily, the astrocyte-to-neuron ratio increases from low vertebrates to rodents and to primates (12). Morphometric analysis of human astrocytes at the cellular level indicates a substantially larger cell body (3-fold larger in diameter) and much more complex processes (10-fold) than those of their rodent counterparts (13). When engrafted neonatally into mice, human glial progenitors can generate astrocytes that retain these distinct human astrocytic morphologies; as adults, the resultant glial chimeric mice can manifest significantly enhanced long-term potentiation and learning (14). But no such assessment of the effects of implanting the adult CNS with astrocytes or their progenitors has yet been performed. Over the time frames studied previously, transplanted human fetal tissue–derived astrocyte progenitors have generally not been observed to exhibit substantial migration, and so the functional contribution of astrocytic addition to the adult CNS has been difficult to assess. As such, there is a critical need for an in vivo model system that allows functional assessment of human astrocytes in the adult CNS.

We have endeavored to build such a model, by taking advantage of the fact that astrocytes slowly turn over in the adult mouse brain (15) and spinal cord (16) and that a fraction of implanted human neural progenitors may remain as progenitor cells for at least a year after transplantation into the rodent CNS (14, 17). We report here that human embryonic stem cell–derived (ESC-derived) and induced pluripotent stem cell–derived (iPSC-derived) neural progenitors, transplanted into the adult mouse spinal cord, gradually replace endogenous astrocytes over a 9-month period, thus creating a "chimeric" spinal cord. This chimeric model was further verified by transplanting progenitors from ALS patient iPSCs, which led to integration of human cells and mouse behavioral deficits.

Conflict of interest: The authors have declared that no conflict of interest exists.
Submitted: August 28, 2014; **Accepted:** December 18, 2014.
Reference information: *J Clin Invest.* doi:10.1172/JCI69097.

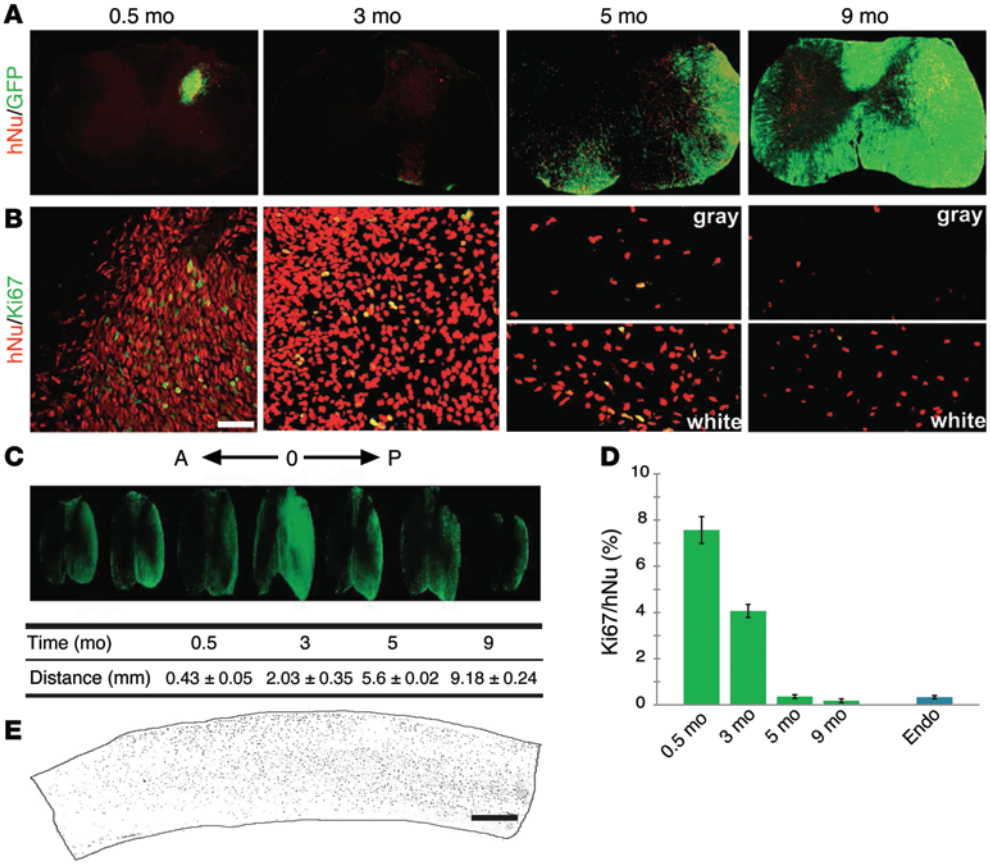

Figure 1. Human cells survive and migrate in the adult spinal cord. (**A**) Distribution of hNu$^+$ and GFP$^+$ cells (from ESCs) in the spinal cord over time (0.5 to 9 months). (**B**) The dividing human cells (from iPSCs) were revealed by Ki67$^+$/hNu$^+$ over time. Scale bar: 50 μm. (**C**) Human cells (marked by GFP) in the spinal cord migrated longitudinally to both rostral (A) and caudal (P) areas, and the distance (mean ± SEM) that hNu$^+$ cells spread in the spinal cord was measured (n = 6), with "0" indicating the injection location. (**D**) Quantification of Ki67$^+$/hNu$^+$ cells (mean ± SEM) in the spinal cord over time. Ki67 expression in the mouse spinal cord was used as an endogenous control (n = 6). (**E**) Longitudinal view of the distribution of hNu$^+$ cells along the spinal cord. Scale bar: 500 μm.

Results

Human cells survive, proliferate, and migrate in the adult mouse spinal cord. To investigate the behaviors of human neural progenitors in the nonneurogenic spinal cord environment, we differentiated GFP-labeled (under the CAG promoter) human ESCs or nonlabeled iPSCs to spinal neural progenitors in the presence of retinoic acid for 35 days (18) and transplanted them into adult mouse cervical spinal cord. A total of 60 mice were transplanted (20 mice with H9-GFP cells, 20 with IMR iPSCs, and 20 with *SOD1*^{D90A} mutant iPSCs). Five transplanted mice were excluded from the study due to reasons unrelated to transplantation, including tumors in the thymus, which the severe combined immunodeficiency (SCID) mice develop. In addition, we excluded animals that did not contain transplanted cells, which was mainly due to technical difficulty in targeting the small mouse spinal cord.

Examination of cross spinal cord sections indicated the presence of GFP (for ESC-derived cells) and human nuclei–positive (hNu$^+$) cells (for both ESC- and iPSC-derived cells) in the spinal cords of grafted animals. Two weeks after transplantation, GFP cells were localized to one side of the spinal cord and were restricted predominantly to the injection site. The GFP cells overlapped completely with those positive for hNu (Figure 1A). Three months after engraftment, hNu$^+$ cells were present beyond the injection site, spreading to adjacent spinal cord. Interestingly, many of the hNu$^+$ cells downregulated GFP at 3 months after transplantation (Figure 1A). Immunostaining revealed that the majority of GFP$^-$ and hNu$^+$ cells were positive for the neuronal marker NeuN (Supplemental Figure 1A; supplemental material available online with this article; doi:10.1172/JCI69097DS1) but not for the glial marker GFAP, suggesting downregulation of GFP in differentiated neurons. From 5 months after transplantation, hNu$^+$ cells occupied nearly the entire injection side of the spinal cord. Some cells were also seen in the contralateral side, especially at the injection segment. At this stage, most hNu$^+$ cells, especially those in the white matter, became GFP$^+$ (Figure 1A). By 9 months, the human cells spread further along the spinal cord, reaching to about 9 mm (9.18 ± 0.24 mm) in length. When viewed in transverse sections, the GFP cells were noted to have spread to both the injection and contralateral sides (Figure 1A). At these later (5 and 9 months) stages, hNu$^+$ cells and GFP cells were largely overlapping in the white matter, whereas some of the cells in the gray matter did not express GFP (Figure 1, A and C). Such a distribution was also seen in sagittal spinal cord sections in which hNu or GFP cells were distributed largely in the white matter (Figure 1E). These results suggest that the grafted human cells have migrated extensively in the adult spinal cord.

Since the transplanted cells were neural progenitors and the grafted cells populated the spinal cord, we examined the dynamics of cell division. Immunostaining for Ki67 together with hNu or GFP indicated that 7.57% ± 0.58% of the human cells were positive for Ki67 at the injection site at 2 weeks after transplantation. At 3 months after transplantation, the Ki67$^+$ cells decreased to 4.07% ± 0.28%. By 5 and 9 months after graft, the Ki67$^+$ cells further decreased to 0.36% ± 0.08% and 0.18%

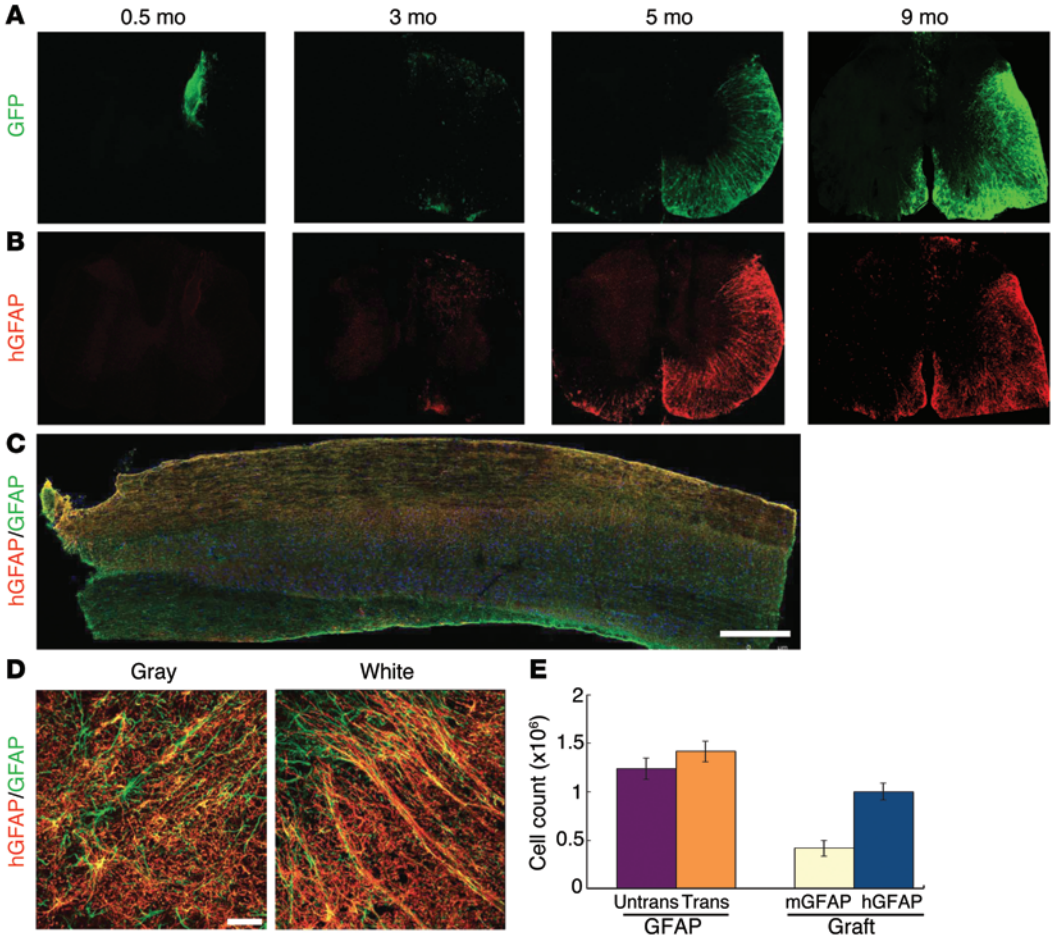

Figure 2. Human neural progenitors differentiate into astrocytes and replace endogenous astrocytes. (**A** and **B**) hGFAP-expressing astrocytes began to appear at 3 months and became the predominant population by 9 months. (**A**) The GFP overlapped with (**B**) hGFAP at 5 and 9 months. (**C**) The longitudinal distribution of hGFAP-expressing astrocytes (red) as well as endogenous astrocytes (green) in the spinal cord. Scale bar: 500 μm. (**D**) Human astrocytes (from iPSCs) in the gray matter and white matter exhibit typical astrocyte morphologies. Scale bar: 50 μm. (**E**) Quantification (mean ± SEM) of all astrocytes ($GFAP^+$) in the transplanted and nontransplanted sides ($n = 3$, $P > 0.05$, t test), and the average population of mouse astrocytes ($GFAP^+/hGFAP^-$) and human astrocytes ($GFAP^+/hGFAP^+$) in the grafted spinal cord at 9 months.

± 0.08%, respectively, similar to the level of endogenous $Ki67^+$ cells population (0.33% ± 0.07%) (Figure 1, B and D). The decrement in neural progenitor mitotic index as a function of time was similar to that noted by Windrem et al., who reported neonatally engrafted tissue-derived human glial progenitor cells, which exhibit a higher mitotic index than that of their murine host until over 6 months in vivo (19). By these later time points, we observed Ki67 cells only in the white matter (Figure 1B). These results suggest that, while many transplanted cells continue to divide in the first 3 months after transplantation, the vast majority become postmitotic by 5 months after transplantation. No tumors or overgrowth were observed in the spinal cords of any of the transplanted animals.

Human neural progenitors differentiate into astrocytes that replace endogenous ones. Human neural progenitors usually produce neurons followed by glia in vitro as well as after transplantation into the developing mouse brain (17). We asked whether the nonneurogenic adult mouse spinal cord environment enhances gliogenesis. Two weeks after graft, the vast majority of the hNu^+ cells retained GFP and expressed nestin. A small population of hNu^+ cells was positive for MAP2 (Supplemental Figure 1C), but no cells were positive for GFAP (Supplemental Figure 1B). At 3 months after engraftment, only a small proportion (5% ± 0.8%) of hNu^+ cells, mostly those localized to the edge of the graft bordering the white matter, expressed human GFAP (hGFAP) and retained GFP (Figure 2, A and B, and Supplemental Figure 1D). From 5 months on, the $hGFAP^+$ cell population among total transplanted cells increased progressively, reaching 38.25% ± 3.86%. The majority of the $GFAP^+$ cells were localized to the white matter in the transplant side, with some contralateral expansion. A small number of hNu^+ cells were $OLIG2^+$ at 3 months (Supplemental Figure 1E) and $NG2^+$ from 5 months after transplantation (Supplemental Figure 1F), suggestive of the oligodendroglial lineage. By 9 months, the $hGFAP^+$ cells occupied nearly the entire transplant side as well as the contralateral white matter (68.5% ± 3.4% of all engrafted cells; Figure 2, A–C). The appearance of $GFAP^+$ cells overlapped with the reappearance of GFP, suggesting that when neural progenitors differentiate to astrocytes, GFP expression is maintained, as previously noted (14, 19). These results indicate that the grafted human neural progenitors exhibit a delayed process of gliogenesis, even in a fundamentally gliogenic environment.

The structural organization of human astrocytes, revealed by the human-specific GFAP antibody and GFP, does not appear to differ from that of endogenous astrocytes, from either cross sections or longitudinal views (Figure 2, A–C). This prompted us to ask whether human astrocytes replace endogenous astrocytes in the normal adult spinal cord. Indeed, the staining for human-specific GFAP almost completely overlapped that for pan-GFAP (for both murine and hGFAP) in the white matter. In the gray matter, the majority of the pan-GFAP cells were also positive for hGFAP, though a small number of the pan-GFAP

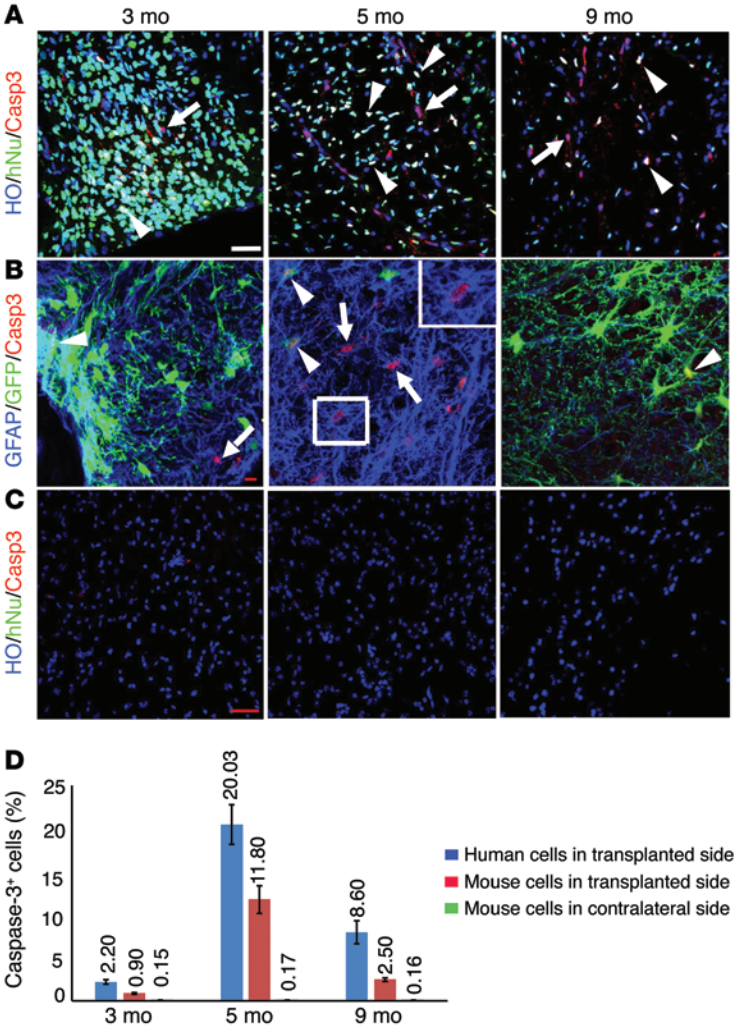

Figure 3. Mouse astrocytes undergo cell death in the adult spinal cord. (**A**) The mouse cells (hNu$^-$) and human cells (hNu$^+$, from iPSCs) were positive for caspase-3 at 3, 5, and 9 months after transplantation. Arrows indicate mouse cells positive for caspase-3; arrowheads indicate human cells positive for caspase-3. Scale bar: 50 μm. HO, Hoechst 33258. (**B**) Mouse astrocytes (GFAP$^+$/GFP$^-$, arrows) and human astrocytes (GFAP$^+$/GFP$^+$, arrowheads, from ESCs) were positive for caspase-3 at 3, 5, and 9 months after transplantation. Scale bar: 10 μm. (**C**) Few mouse cells in untransplanted side were positive for caspase-3 at 3, 5 and 9 months. Scale bar: 50 μm. (**D**) Quantification of caspase-3–positive populations (mean ± SEM) (numbers above bars) in human (hNu$^+$) and mouse (hNu$^-$) cells in transplanted side and contralateral side at 3, 5, and 9 months (n = 3).

cells were not labeled with hGFAP, suggestive of mouse origin of these cells (Figure 2D). Quantitative analysis of the total astrocytes (as defined by the pan-GFAP antibody and Hoechst labeling) in the grafted spinal cord at 9 months indicated that total astrocyte numbers did not significantly differ between nontransplanted and transplanted spinal cords ($1.24 \pm 0.06 \times 10^6$ vs. $1.42 \pm 0.06 \times 10^6$; Figure 2E). However, measurement of human astrocytes in the transplanted cord, as defined by hGFAP, revealed that 71% ± 7.5% of all GFAP$^+$ cells were of human origin (hGFAP$^+$/pan-GFAP$^+$; Figure 2, C and E). At the center of the transplanted site, nearly all the GFAP$^+$ cells expressed hGFAP immunoreactivity (97.8%). These results suggest that human astrocytes gradually replace their endogenous murine counterparts following transplantation of neural progenitors into the adult mouse spinal cord.

The fact that the human astrocytes organize into a structure that is indistinguishable from the mouse counterparts could indicate a fusion of grafted human cells with endogenous astrocytes. The possibility of cell fusion was also lately reported when using human ESC–derived neural progenitors (20). Confocal analysis indicated that the GFP$^+$ cell did not contain additional nuclei besides the hNu$^+$ nucleus (Supplemental Figure 2A). The GFP$^+$ cells were not positive for the mouse-specific antibody M2/M6 (Supplemental Figure 2B), and in the transplanted side, the M2/M6 fluorescent signal was substantially lower than that in the nontransplanted side, especially in the white matter (Supplemental Figure 2, C and D). Together, these results corroborate our conclusion that human astrocytes replace rather than fuse with endogenous mouse astrocytes.

Astrocytes undergo cell death in the adult mouse spinal cord. The replacement of mouse astrocytes by newly produced human astrocytes suggests that mouse astrocytes would die over time. Previous studies indicate that in the adult brain glial cells slowly turn over at a daily rate of 0.4% for astrocytes (15). Using caspase-3 staining, we found caspase-3–expressing cells in the transplanted spinal cord. To identify the source of dying cells, we colabeled the cords with caspase-3 and hNu. We found that about 0.9% ± 0.1%, 11.8% ± 1.5%, and 2.5% ± 0.1% of the mouse cells (hNu$^-$) in the transplanted side were positive for caspase-3 at 3, 5, and 9 months after transplantation, respectively (Figure 3, A and D). Interestingly, we also observed that a substantial proportion of human cells expressed caspase-3 during the same period, 2.2% ± 0.1%, 20.03% ± 2.8%, and 8.6% ± 0.9% for 3, 5, and 9 months after transplantation, respectively (Figure 3, A and D). We then asked what types of mouse and human cells undergo cell death. Costaining of caspase-3 with MAP2 or GFAP revealed that the caspase-3–expressing mouse cells (GFP$^-$, hNu$^-$) were almost exclusively GFAP$^+$ (Figure 3B), indicating ongoing loss of mouse astrocytes. Among the human cells (GFP$^+$, hNu$^+$), both GFAP$^+$ astrocytes and MAP2$^+$ neurons expressed caspase-3 (Figure 3B and Supplemental Figure 3A), suggesting that the extra human neurons and astrocytes in the spinal cord may be eliminated through apoptosis. In the contralateral side where few human astrocytes were present or untransplanted spinal cord, few caspase-3–positive mouse cells (hNu$^-$) were observed (Figure 3, C and D). Together, these results indicate an increased loss of mouse astrocytes at the time (5 and 9 months) that is coincident with the generation of new human astrocytes from grafted progenitors.

Human astrocytes structurally integrate into the host tissue. The gross structure of the transplanted mouse spinal cord was not altered (Figure 1 and Figure 2C). Cross sections of the grafted cord exhibited indistinguishable structures from the nontransplanted cord (Figures 1 and 2). We asked whether the human astrocytes behave like their mouse counterparts. In the

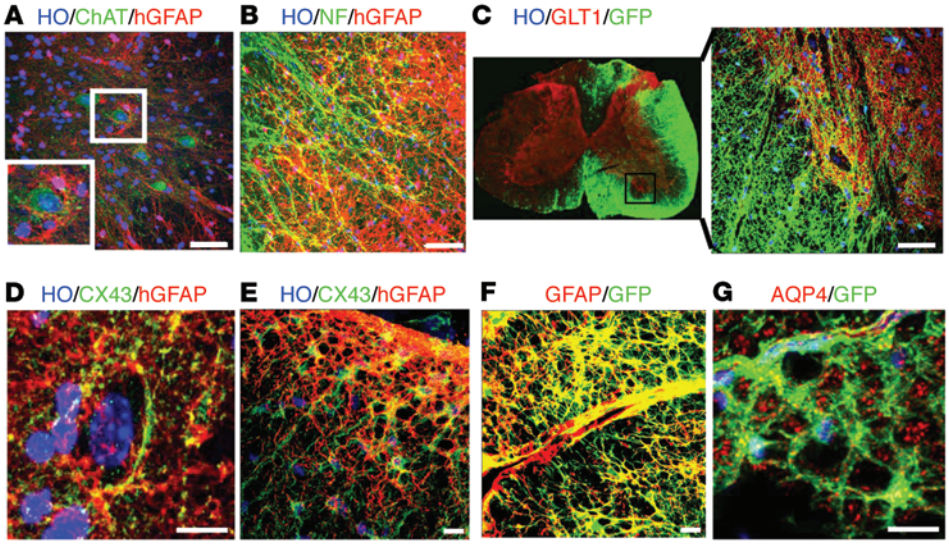

Figure 4. Human astrocytes structurally integrate into the host tissue. (**A**) In the gray matter, the hGFAP$^+$ astrocytes (from iPSCs) presented with a star-shaped morphology, surrounding neurons, including ChAT$^+$ MNs (inset). (**B**) In the white matter, the human astrocytes (from iPSCs) extended long processes that line up with the neurofilament-positive (NF$^+$) axons. (**C**) The distribution of GLT1 is similar between the transplanted side and the untransplanted side, with a higher density in the gray matter than in the white matter. (**D**) In the gray matter, CX43 was predominantly in the hGFAP$^+$ astrocyte processes, especially in the area surrounding neuronal cell bodies. (**E**) In the white matter, CX43 immunoreactivity was present in the cytoplasm. (**F**) Human astrocytes (GFP$^+$/GFAP$^+$, from ESCs) projected to the blood vessel, with their end feet closely surrounding the blood vessel. (**G**) The AQP4 signals were largely concentrated on the astrocytic end feet along the vessels. Scale bar: 50 μm (**A**–**C**); 10 μm (**D**–**G**).

gray matter, the hGFAP$^+$ astrocytes exhibited larger cell bodies with more processes than endogenous astrocytes (Supplemental Figure 4, A and B). The hGFAP$^+$ cells presented with a star-shaped morphology, surrounding neurons, including ChAT$^+$ motor neurons (MNs) (Figure 4A). In the white matter, the human astrocytes extended long processes that line up with neurofilament-positive axons (Figure 4B). Thus, morphological differentiation of human astrocytes coincides with the local spinal cord environment.

One of the best-known functions of astrocytes is to buffer neurotransmitters that are released during neural excitation. Glutamate transporters (GLT), especially GLT1 (also known as EAAT2 in humans), are highly expressed in astrocytes (21, 22). Immunostaining indicated that the distribution of GLT1 was not altered in the transplanted side as compared with that in the untransplanted side, with a higher density in the gray matter than in the white matter (Figure 4C). The grafted human astrocytes in the white matter exhibited a weaker GLT1 staining than those in the gray matter. Interestingly, the GLT1 signals were concentrated in the processes of human astrocytes in the gray matter that appose neuronal cell bodies (Figure 4C), suggesting an intimate relationship between the grafted human astrocytes and endogenous mouse neurons.

Another feature of astrocytes is their numerous gap junctions through which ions and small molecules can move freely, a structural basis for cell-cell lactate shuttle (3, 4). The predominant connexin in astrocytes is CX43. Coinciding with the appearance of GFAP-expressing astrocytes, CX43 appeared in human cells at 5 months after transplantation, exhibiting a punctate membrane staining pattern in the human (hGFAP$^+$) astrocytes in the gray matter and white matter. In the gray matter, CX43 was predominantly in the hGFAP$^+$ astrocyte processes, especially in the area surrounding neuronal cell bodies (Figure 4D). In the white matter, CX43 immunoreactivity was also present in the cytoplasm (Figure 4E). This expression pattern of CX43 in human astrocytes is similar to that in the endogenous mouse astrocytes as well as that reported in the rat spinal cord (23).

Another critical role of astrocytes is shuttling molecules between the circulation and the brain parenchyma through participation in the gliovascular unit. Indeed, human astrocytes projected to blood vessels, with their end feet closely surrounding the blood vessel (Figure 4F). The water channel, aquaporin 4 (AQP4), which enables fast water influx or efflux and thus maintains the osmotic balance in the CNS (24), was also expressed on the end feet of human astrocytes along the vessels (Figure 4G). Together, these results suggest that human astrocytes are at least structurally integrated into the host spinal cord.

Astrocytes derived from ALS patient iPSCs integrate in the spinal cord and result in mouse functional deficit. Astrocytes play important roles in the pathogenesis of neurodegenerative diseases (25). Astrocytes isolated from ALS transgenic mice or patients with ALS have been shown to be toxic to MNs in culture (6, 26–28), and astrocytes carrying the superoxide dismutase 1 ($SOD1^{G93A}$) mutation exacerbate the degeneration process of MNs in vivo (10). To determine whether astrocytes derived from ALS patient iPSCs may affect mouse neurons, we transplanted neural progenitors that were derived from ALS ($SOD1^{D90A}$) patient iPSCs (29). Similar to WT astrocytes, ALS astrocytes migrated widely longitudinally and laterally along the spinal cord, with a similar density 9 months after transplantation (Figure 5A), and they exhibited typical astrocyte morphologies, depending on their locations in the white matter or gray matter (Figure 5B). They similarly wrapped neurons in the gray matter, lined up with nerve fibers in the white matter, exhibited characteristic distribution of GLT1 in gray versus white matter, and connected blood vessels through their end feet (Supplemental Figure 5, A–D). In particular, the ALS astrocytes exhibited larger cell bodies and thicker processes as well as a higher level of GFAP, as measured by densitometry, than non-ALS astrocytes (Supplemental Figure 5, E and F). Stereological analysis indicated a (40%) reduced number of endogenous MN in the $SOD1^{D90A}$ astrocyte transplantation group as compared with that in the WT astrocyte group (Figure 5, C and D). In addition, the MNs in $SOD1^{D90A}$ astrocyte-transplanted group showed

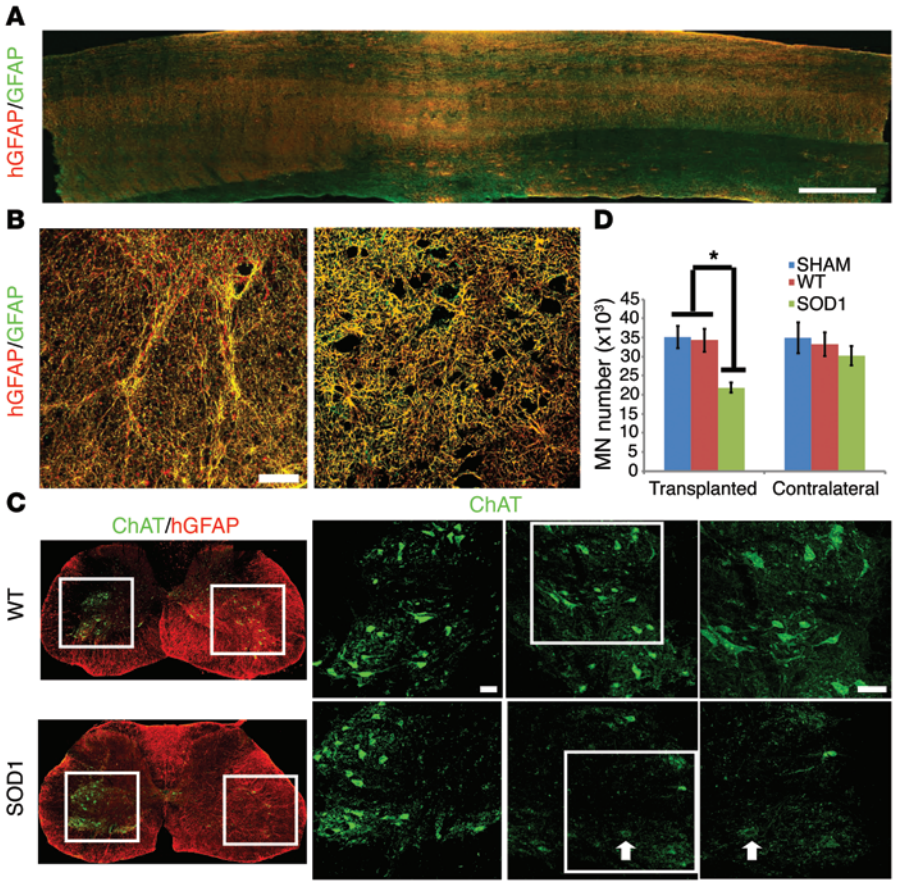

Figure 5. Integration of astrocytes from patients with ALS and its effect on mouse MNs. (**A**) Longitudinal distribution of hGFAP-expressing astrocytes (red) as well as endogenous astrocytes (green) in the spinal cord. Scale bar: 500 μm. (**B**) Human astrocytes (from iPSCs) in the gray matter and white matter exhibit typical astrocyte morphologies. Scale bar: 50 μm. (**C**) Mouse MNs decreased in number in the ALS astrocyte–transplanted group compared with those in the WT astrocyte group. ChAT$^+$ cells in the boxed regions of the ChAT/hGFAP images are magnified to their right, and the boxed ChAT images are further magnified to their right; arrows indicates a MN with lower ChAT intensity. Scale bar: 50 μm. (**D**) Quantification of mouse MNs (mean ± SEM) on the transplanted versus contralateral side (n = 6, $^*P < 0.05$, 1-way ANOVA followed by Tukey's multiple comparison tests).

decreased choline acetyltransferase (ChAT) staining compared with those in the contralateral side and WT group (Figure 5C), suggesting degenerative change. Neuronal degeneration and/or astrocyte reaction often induce microglial activation, as seen in *G93A* transgenic mice (30). Interestingly, however, no obvious morphological sign of microglial activation was discerned in the spinal cord transplanted with ALS neural progenitors (data not shown).

To discern potential functional impact of grafted human astrocytes, we examined locomotion behaviors of transplanted mice by grip strength and treadmill analyses. Mice transplanted with WT astrocytes showed no obvious difference, as compared with those that underwent sham surgery (transplanted with CSF) (Figure 6). In contrast, the forelimbs of mice that received ALS astrocyte transplant exhibited decreased grip strength, stride length, and print area as well as decreased longitudinal deviation and increased stance time when compared with those that received transplant with WT astrocytes and CSF (sham surgery) (Figure 6; $P < 0.05$). Thus, human astrocytes not only structurally but also functionally integrate into the adult spinal cord.

Discussion

Investigation of the roles of human astrocytes is largely based on in vitro systems. Cell cultures often subject astrocytes to artificial conditions and segregate them from neurons, other glial cells, and blood vessels. At present, understanding the roles of human astrocytes in the homeostatic or diseased CNS is severely hindered by the near complete lack of in vivo model systems. By taking advantage of the maintenance of the progenitor state of human neural precursors over a period of time, we have created a "chimeric" model through a simple transplantation step. The most striking feature of the model is the integration of human cells into the host tissue, which is structurally indistinguishable from the nontransplanted tissue. The human astrocytes retain the hominid features in the mouse spinal cord, exhibiting large cell bodies with more processes. Yet they "hug" mouse neurons in the gray matter and line up with axons in the white matter. Even the expression patterns of some potential functional molecules, such as GLT1, resemble those in endogenous astrocytes. The human astrocytes residing in the gray matter express a higher level of GLT than those sitting in the white matter. They also participate in the vasculature system by wrapping around blood vessels with their processes. The functional implication of grafted human astrocytes is demonstrated by the effects of ALS astrocytes on neighboring host neurons and mouse locomotion behaviors. The degree of chimera depends on the time during which the human cells undergo differentiation and the distance from which the human progenitors were introduced. The longer period after transplantation and/or the closer to the graft site, the more complete the replacement by the human astrocytes. This creates a gradient of replacement, allowing assessment of the relative contribution of human astrocytes in the spinal cord. In that regard, one may "visualize" a dynamic relationship between human astrocytes and host cells/tissues in a single spinal cord.

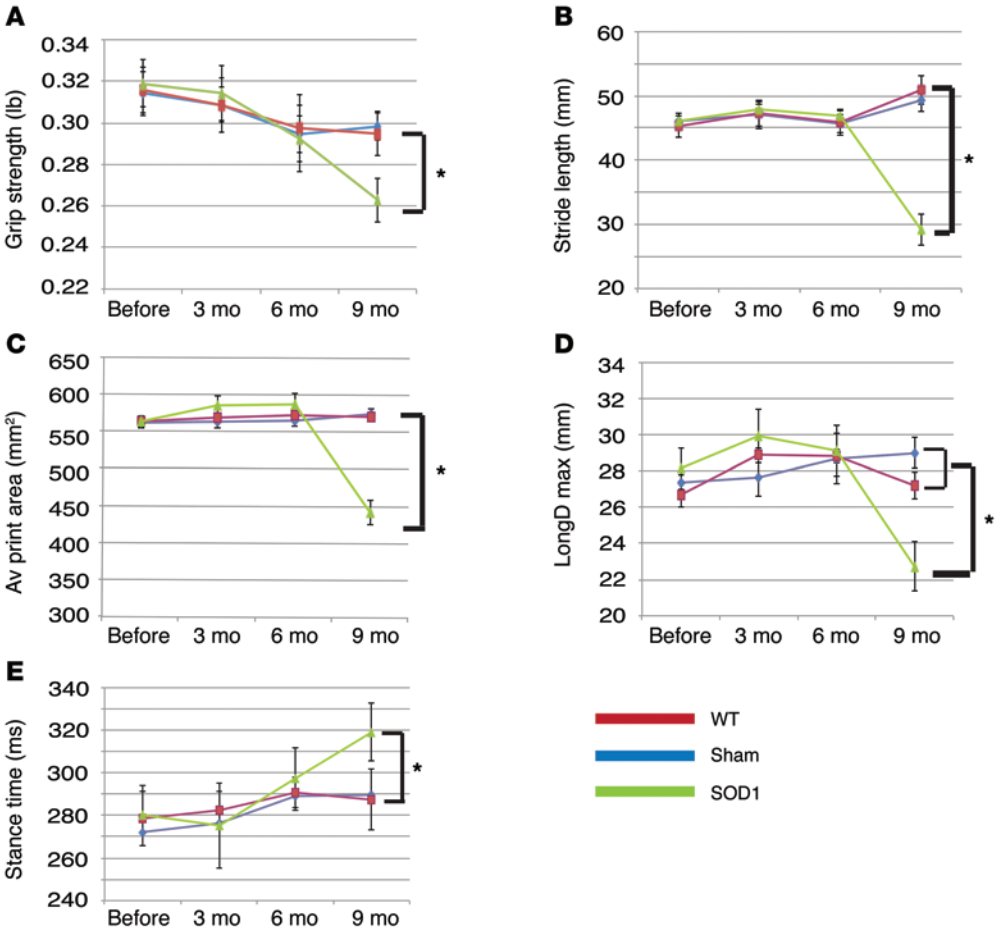

Figure 6. Transplantation of astrocytes from patients with ALS results in mouse movement deficits. (**A**) Mice receiving ALS astrocyte transplant show decreased grip strength (mean ± SEM) at 9 months after transplantation, as compared with those receiving WT astrocyte transplant (n = 6, *P < 0.05, 1-way ANOVA followed by Tukey's multiple comparison tests). (**B**–**E**) Treadscan analysis reveals (**B**) decreased stride length, (**C**) average print area, (**D**) decreased maximum longitudinal deviation, and (**E**) increased stance time in mice receiving ALS astrocyte transplant, as compared with those receiving WT astrocyte transplant (n = 6, *P < 0.05, 1-way ANOVA followed by Tukey's multiple comparison tests). Data represent mean ± SEM.

Technically, we chose to target the spinal cord as it is structurally simple and there is a clear demarcation between gray matter and white matter. This enables us to measure cell migration/integration in a quantitative manner and allows us to observe the behaviors of astrocytes in gray versus white matter. Another rationale behind this choice is the nonneurogenic environment, which potentially enhances astroglial differentiation. Another technical consideration is the choice of donor cells. We have chosen neural progenitors that are patterned to the cervical spinal cord region with retinoic acid (31), as the regional identity of astrocytes is largely determined when their progenitors are patterned (32, 33). We also used neural progenitors that were differentiated from human ESCs and iPSCs for 35 days, a relatively early stage (for human cells). Forebrain neural progenitors at that early stage often produce large isolated grafts in the mouse or rat brain (34, 35). When transplanted into the adult neurogenic region, such as the dentate gyrus, forebrain progenitors also proliferate for a period of time (36). It is thus very interesting to observe that the spinal progenitors migrate extensively, differentiate to astrocytes efficiently, and integrate into the cord structurally. We reason that the lack of overgrowth or tumor formation by the early human neural progenitors is likely due to the spinal fate of the human neural progenitors and the nonneurogenic cord environment.

Our observation that mouse astrocytes undergo cell death and are replaced by newly born human astrocytes also reveals that astrocytes in the stable CNSs of mice, perhaps also in other animals including humans, undergo regular turnover. This finding is in line with a previous study using ^{3}H labeling that indicated an as high as 0.4% daily incorporation rate of new astrocytes in adult (9 months) mouse brain (15) or BrdU incorporation in rat spinal cord (16), suggesting a potentially similar rate of cell loss to maintain the homeostasis. We indeed observed death of mouse astrocytes through labeling with cleaved caspase-3 and the presence of large numbers of human astrocytes that do not fuse to mouse cells. The reason for the increased proportion of caspase-3 mouse astrocytes at 5 and 9 months after transplantation is not known. It, however, coincides with the production of new human astrocytes from the grafted neural progenitors. Despite unknown mechanisms, transplantation of human neural progenitors into the mouse spinal cord offers an opportunity to create versatile "chimeric" models to assess the roles of human astrocytes in disease progression and/or therapeutic contribution. An analogous chimeric model was reported by which human oligodendroglial progenitor cells replace their mouse counterparts when transplanted into the hypomyelinated neonatal mouse brain, in which the normal human glial progenitors compete with the myelin-deficient host progenitors to myelinate the recipient CNS (19, 37). Similarly, human glial progenitor cells introduced into the normal neonatal brain also yield mice with forebrains chimeric for astrocytes and their progenitors, and this chimerization may be so extensive as to influence synaptic plasticity and cognitive processing in the recipient mice (14). In contrast to these studies, our

present study shows for what we believe to be the first time that the CNS of adult animals may similarly be rendered chimeric for human and mouse glia, following direct introduction of neural progenitor cells into the mature spinal cord.

Astrocytes are increasingly recognized as crucial contributors to the pathogenesis/progression of neurological conditions, including ALS (38), Rett syndrome (8), and Huntington disease (39). Our present study suggests that human neural cells, especially astrocytes derived from *SOD1* mutant iPSCs impair neighboring neurons, leading to functional deficits in mice. We do not exclude the possible functional contribution from other neural cells that are differentiated from the grafted neural progenitors, including neurons and oligodendrocytes. This finding is in line with observations made using astrocytes isolated from ALS transgenic mice or patients with ALS (6, 7, 26). More importantly, the results from our ALS cell transplant study demonstrate functional integration of human astrocytes in our chimeric model. Hence, our model would allow dissection of the contribution of disease astrocytes in the intact animal environment when using neural or astrocyte progenitors from iPSCs with neurological conditions, as illustrated by using rodent primary astrocytes (10). Along the same line, transplantation of healthy human neural (astrocyte) progenitors into the diseased CNS should permit assessment of the potential therapeutic value of astrocytes. Indeed, transplantation of rat glial progenitors to the spinal cords of ALS mice appears to neutralize the toxicity of endogenous astrocytes, thereby extending the life span of the mice (40). Transplantation of glial progenitors alleviates disease progression in the Huntington model (41). Furthermore, the human neural progenitors may be further engineered to deliver therapeutic molecules, permitting the effective delivery of these molecules throughout the CNS. Thus, this simple model opens new possibilities for investigating the functions of human astrocytes in the intact CNS.

Methods

Human neural progenitors

Human neural progenitors were differentiated for 35 days from ESCs (H9 line, passage 21) or iPSCs (IMR-90-4 and superoxide dismutase [*SOD1*^{D90A}] mutant lines passages 21 and 25). The H9 ESC line was labeled with GFP under the ubiquitous promoter CAG (42). Since astrocytes in different brain regions exhibit differential functional attributes (43) and astrocytes differentiated from PSCs also carry regional identities (33), we differentiated the PSCs to ventral spinal progenitors according to our protocol for spinal MN differentiation(31). The PSCs were first differentiated to neuroepithelia for 8 days, followed by treatment with retinoic acid (0.1 μM) and purmorphamine (a sonic hedgehog agonist, 1 μM) from day 10 to 23 to pattern the cells to ventral spinal progenitors. The progenitors were then expanded in the presence of fibroblast growth factor 2 until day 35 for transplantation. Nearly all the progenitors expressed Sox1 and HoxB4 and most of them (80%) expressed Olig2 (31).

Cell transplantation and tissue preparation

Adult SCID (NOD/SCID) mice, aged 8–10 weeks, were obtained from The Jackson Laboratory and anesthetized with 1.5% isoflurane with oxygen and fixed in a stereotaxic frame. A total of 5×10^4 neural progenitors (in 0.5~1 μl CSF) were transplanted into the right side of C5-C6 cervical spinal cord using a glass micropipette, with a tip diameter of about 50 μm that was attached to a stereotaxic device. Animals in the sham (control) group received injection of the same amount of CSF (without cells). The injection site was marked by charcoal before the wound was sutured.

At 1 to 2 weeks (referred to as 0.5 months), 3, 5, and 9 months after transplantation, 6 to 11 mice were overdosed with pentobarbital (250 mg/kg, i.p.) and perfused transcardially with 0.9% sodium chloride, followed by 4% paraformaldehyde. The spinal cords were removed and post fixed in 4% paraformaldehyde for 4 hours, followed by dehydration in 20% and 30% sucrose solution. The specimens were cut into 20-μm-thick consecutive free-floating cross sections using a microtome.

Immunocytochemistry and quantification

Free-floating sections were washed in PBS 3 times and then blocked in PBS/0.2% Triton X-100/10% donkey serum for 1 hour. The sections were incubated in the primary antibodies (Supplemental Table 1) overnight at 4°C. After being rinsed in PBS (3 times for 10 minutes each time), they were incubated with fluorescein-conjugated secondary antibodies for 1 hour at room temperature. Hoechst 33258 (1:1,000) was added for 5 minutes to label nuclei.

Images were collected with a Nikon TE600 fluorescence microscope (Nikon Instruments) or a Nikon C1 laser-scanning confocal microscope (Nikon). For comparing the GFAP immunofluorescent intensity, we measured the mean gray value of hGFAP staining using ImageJ. The populations of Ki67$^+$, caspase-3$^+$, and GFAP$^+$ cells were counted in fields chosen by an automated stage movement operated by Stereo Investigator software (MicroBrightField Inc.) or using Z-section images analyzed using ImageJ software. Briefly, the number of grafted human cells (hNu$^+$) and proliferating cells (Ki67$^+$) was counted with StereoInvestigator software (MicroBrightField Inc.) on every 6 sections as described previously (44). The area of the graft was outlined according to the presence of hNu$^+$ cells under a ×10 objective of a Zeiss fluorescent scope. Cell counting was performed with a ×40 objective in fields chosen by the software. The number of cells on each section and within the whole graft was estimated by the Stereo Investigator software (45). We used 3 mice at 0.5, 3, and 5 months and 6 mice at 9 months in each group for quantification. Data are presented as mean ± SEM. Human astrocytes were identified either by human-specific GFAP antibody (STEM123) or double labeling for GFAP with GFP or hNu, whereas mouse astrocytes were determined by GFAP immunostaining without expression of hNu. The apoptotic human and mouse cells were marked by immunostaining for caspase-3 in conjunction with hNu (for humans) or M2/M6 (for mice) staining.

Behavior tests

Six mice per group that lived for 9 months after surgery were used for behavior tests. Behavioral tests were conducted before and after transplantation every 2 months until the animals were sacrificed.

Grip strength. The grip strength test measures forepaw strength. Animals were allowed to grasp the grip strength meter grid with their forepaws and then pulled gently from the base of the tail until they released the grid. The test was repeated 5 times for each mouse.

TreadScan analysis. TreadScan (Columbus Instruments) is an unbiased device to detect gait alterations. All mice were allowed to walk on

the motor-driven treadmill belt at a speed of 11 cm/s for a period of 20 seconds as we described previously (44). The digital data (footprints and body movement) were analyzed by TreadScan software (CleverSys), and each of the parameters was compared between ipsilateral and contralateral sides and between the transplant and nontransplant groups.

Statistics

Results were expressed as mean ± SEM unless otherwise indicated. For simple comparisons, paired 2-tailed *t* tests were applied; for multiple group comparisons, 1-way ANOVA, followed by Tukey's multiple comparison tests, was used to compare among groups. A *P* value of less than 0.05 was considered significant.

Study approval

All protocols involving animals were approved by the University of Wisconsin IACUC.

Acknowledgments

We thank Jeff Rothstein of Johns Hopkins for providing the GLT1 antibody. This study was supported in part by the NIH (NS045926, NS057778, and MH099587), the Bleser Family Foundation, the Busta Foundation, the Eunice Kennedy Shriver National Institute of Child Health and Human Development (P30 HD03352), and the National Natural Science Foundation of China (NSFC 81471302).

Address correspondence to: Hong Chen, Department of Rehabilitation of Tongji Hospital, Tongji Medical College, Huazhong University of Science and Technology, Wuhan, China. Phone: 86.027.83663372; E-mail: chenhong1129@hotmail.com. Or to: Su-Chun Zhang, Waisman Center, University of Wisconsin, 1500 Highland Avenue, Madison, Wisconsin, USA. Phone: 608.265.2543; E-mail: zhang@waisman.wisc.edu.

1. Eroglu C, Barres BA. Regulation of synaptic connectivity by glia. *Nature*. 2010;468(7321):223–231.
2. Pannasch U, et al. Astroglial networks scale synaptic activity and plasticity. *Proc Natl Acad Sci U S A*. 2011;108(20):8467–8472.
3. Rouach N, Koulakoff A, Abudara V, Willecke K, Giaume C. Astroglial metabolic networks sustain hippocampal synaptic transmission. *Science*. 2008;322(5907):1551–1555.
4. Benediktsson AM, et al. Neuronal activity regulates glutamate transporter dynamics in developing astrocytes. *Glia*. 2012;60(2):175–188.
5. Brenner M, Johnson AB, Boespflug-Tanguy O, Rodriguez D, Goldman JE, Messing A. Mutations in GFAP, encoding glial fibrillary acidic protein, are associated with Alexander disease. *Nat Genet*. 2001;27(1):117–120.
6. Marchetto MC, Muotri AR, Mu Y, Smith AM, Cezar GG, Gage FH. Non-cell-autonomous effect of human SOD1 G37R astrocytes on motor neurons derived from human embryonic stem cells. *Cell Stem Cell*. 2008;3(6):649–657.
7. Di Giorgio FP, Carrasco MA, Siao MC, Maniatis T, Eggan K. Non-cell autonomous effect of glia on motor neurons in an embryonic stem cell-based ALS model. *Nat Neurosci*. 2007;10(5):608–614.
8. Ballas N, Lioy DT, Grunseich C, Mandel G. Non-cell autonomous influence of MeCP2-deficient glia on neuronal dendritic morphology. *Nat Neurosci*. 2009;12(3):311–317.
9. Bradford J, Shin JY, Roberts M, Wang CE, Li XJ, Li S. Expression of mutant huntingtin in mouse brain astrocytes causes age-dependent neurological symptoms. *Proc Natl Acad Sci U S A*. 2009;106(52):22480–22485.
10. Papadeas ST, Kraig SE, O'Banion C, Lepore AC, Maragakis NJ. Astrocytes carrying the superoxide dismutase 1 (SOD1G93A) mutation induce wild-type motor neuron degeneration in vivo. *Proc Natl Acad Sci U S A*. 2011;108(43):17803–17808.
11. Verkhratsky A, et al. Neurological diseases as primary gliopathies: a reassessment of neurocentrism. *ASN Neuro*. 2012;4(3):e00082.
12. Sherwood CC, et al. Evolution of increased glia-neuron ratios in the human frontal cortex. *Proc Natl Acad Sci U S A*. 2006;103(37):13606–13611.
13. Oberheim NA, et al. Uniquely hominid features of adult human astrocytes. *J Neurosci*. 2009;29(10):3276–3287.
14. Han X, et al. Forebrain engraftment by human glial progenitor cells enhances synaptic plasticity and learning in adult mice. *Cell Stem Cell*. 2013;12(3):342–353.
15. McCarthy GF, Leblond CP. Radioautographic evidence for slow astrocyte turnover and modest oligodendrocyte production in the corpus callosum of adult mice infused with 3H-thymidine. *J Comp Neurol*. 1988;271(4):589–603.
16. Horner PJ, et al. Proliferation and differentiation of progenitor cells throughout the intact adult rat spinal cord. *J Neurosci*. 2000;20(6):2218–2228.
17. Guillaume DJ, Johnson MA, Li XJ, Zhang SC. Human embryonic stem cell-derived neural precursors develop into neurons and integrate into the host brain. *J Neurosci Res*. 2006;84(6):1165–1176.
18. Li XJ, et al. Specification of motoneurons from human embryonic stem cells. *Nat Biotechnol*. 2005;23(2):215–221.
19. Windrem MS, et al. Progenitor cells derived from the adult human subcortical white matter disperse and differentiate as oligodendrocytes within demyelinated lesions of the rat brain. *J Neurosci Res*. 2002;69(6):966–975.
20. Cusulin C, et al. Embryonic stem cell-derived neural stem cells fuse with microglia and mature neurons. *Stem Cells*. 2012;30(12):2657–2671.
21. Rothstein JD, et al. Localization of neuronal and glial glutamate transporters. *Neuron*. 1994;13(3):713–725.
22. Storck T, Schulte S, Hofmann K, Stoffel W. Structure, expression, and functional analysis of a Na(+)-dependent glutamate/aspartate transporter from rat brain. *Proc Natl Acad Sci U S A*. 1992;89(22):10955–10959.
23. Ochalski PA, Frankenstein UN, Hertzberg EL, Nagy JI. Connexin-43 in rat spinal cord: localization in astrocytes and identification of heterotypic astro-oligodendrocytic gap junctions. *Neuroscience*. 1997;76(3):931–945.
24. Iliff JJ, et al. A paravascular pathway facilitates CSF flow through the brain parenchyma and the clearance of interstitial solutes, including amyloid β. *Sci Transl Med*. 2012;4(147):147ra111.
25. Serio A, et al. Astrocyte pathology and the absence of non-cell autonomy in an induced pluripotent stem cell model of TDP-43 proteinopathy. *Proc Natl Acad Sci U S A*. 2013;110(12):4697–4702.
26. Haidet-Phillips AM, et al. Astrocytes from familial and sporadic ALS patients are toxic to motor neurons. *Nat Biotechnol*. 2011;29(9):824–828.
27. Meyer K, et al. Direct conversion of patient fibroblasts demonstrates non-cell autonomous toxicity of astrocytes to motor neurons in familial and sporadic ALS. *Proc Natl Acad Sci U S A*. 2014;111(2):829–832.
28. Nagai M, et al. Astrocytes expressing ALS-linked mutated SOD1 release factors selectively toxic to motor neurons. *Nat Neurosci*. 2007;10(5):615–622.
29. Chen H, et al. Modeling ALS with iPSCs reveals that mutant SOD1 misregulates neurofilament balance in motor neurons. *Cell Stem Cell*. 2014;14(6):796–809.
30. Alexianu ME, Kozovska M, Appel SH. Immune reactivity in a mouse model of familial ALS correlates with disease progression. *Neurology*. 2001;57(7):1282–1289.
31. Li XJ, et al. Directed differentiation of ventral spinal progenitors and motor neurons from human embryonic stem cells by small molecules. *Stem Cells*. 2008;26(4):886–893.
32. Hochstim C, Deneen B, Lukaszewicz A, Zhou Q, Anderson DJ. Identification of positionally distinct astrocyte subtypes whose identities are specified by a homeodomain code. *Cell*. 2008;133(3):510–522.
33. Krencik R, Weick JP, Liu Y, Zhang ZJ, Zhang SC. Specification of transplantable astroglial subtypes from human pluripotent stem cells. *Nat Biotechnol*. 2011;29(6):528–534.
34. Aubry L, Bugi A, Lefort N, Rousseau F, Peschanski M, Perrier AL. Striatal progenitors derived from human ES cells mature into DARPP32 neurons in vitro and in quinolinic acid-lesioned rats. *Proc Natl Acad Sci U S A*. 2008;105(43):16707–16712.
35. Roy NS, Cleren C, Singh SK, Yang L, Beal MF, Goldman SA. Functional engraftment of human ES cell-derived dopaminergic neurons enriched by coculture with telomerase-immortalized midbrain astrocytes. *Nat Med*. 2006;12(11):1259–1268.
36. Liu Y, et al. Medial ganglionic eminence-like

cells derived from human embryonic stem cells correct learning and memory deficits. *Nat Biotechnol*. 2013;31(5):440–447.
37. Sim FJ, McClain CR, Schanz SJ, Protack TL, Windrem MS, Goldman SA. CD140a identifies a population of highly myelinogenic, migration-competent and efficiently engrafting human oligodendrocyte progenitor cells. *Nat Biotechnol*. 2011;29(10):934–941.
38. Clement AM, et al. Wild-type nonneuronal cells extend survival of SOD1 mutant motor neurons in ALS mice. *Science*. 2003;302(5642):113–117.
39. Shin JY, Fang ZH, Yu ZX, Wang CE, Li SH, Li XJ. Expression of mutant huntingtin in glial cells contributes to neuronal excitotoxicity. *J Cell Biol*. 2005;171(6):1001–1012.
40. Lepore AC, et al. Focal transplantation-based astrocyte replacement is neuroprotective in a model of motor neuron disease. *Nat Neurosci*. 2008;11(11):1294–1301.
41. Benraiss A, et al. Sustained mobilization of endogenous neural progenitors delays disease progression in a transgenic model of Huntington's disease. *Cell Stem Cell*. 2013;12(6):787–799.
42. Xia X, Ayala M, Thiede BR, Zhang SC. In vitro- and in vivo-induced transgene expression in human embryonic stem cells and derivatives. *Stem Cells*. 2008;26(2):525–533.
43. Tsai HH, et al. Regional astrocyte allocation regulates CNS synaptogenesis and repair. *Science*. 2012;337(6092):358–362.
44. Ma L, et al. Human embryonic stem cell-derived GABA neurons correct locomotion deficits in quinolinic acid-lesioned mice. *Cell Stem Cell*. 2012;10(4):455–464.
45. Yang D, Zhang ZJ, Oldenburg M, Ayala M, Zhang SC. Human embryonic stem cell-derived dopaminergic neurons reverse functional deficit in parkinsonian rats. *Stem Cells*. 2008;26(1):55–63.